Journal of Materials Chemistry A

COMMUNICATION

View Article Online
View Journal | View Issue

Cite this: J. Mater. Chem. A, 2016, 4, 6259

Received 22nd January 2016
Accepted 30th March 2016

DOI: 10.1039/c6ta00638h

www.rsc.org/MaterialsA

Covalent triazine-based frameworks (CTFs) from triptycene and fluorene motifs for CO_2 adsorption†

Subarna Dey,[a] Asamanjoy Bhunia,[a] Dolores Esquivel[b] and Christoph Janiak*[a]

Two microporous covalent triazine-based frameworks (CTFs) with triptycene (TPC) and fluorene (FL) backbones have been synthesized through a mild $AlCl_3$-catalyzed Friedel–Crafts reaction, with the highest surface area of up to 1668 $m^2\ g^{-1}$ for non-ionothermal CTFs. CTF-TPC and CTF-FL show an excellent carbon dioxide uptake capacity of up to 4.24 mmol g^{-1} at 273 K and 1 bar.

The burning of fossil fuels increases the CO_2 level in the atmosphere which may contribute to global warming and is more imminent to ocean acidification.[1,2] Therefore, research on carbon capture and storage/sequestration (CCS) has been receiving great attention over the last few decades.[3] It may be necessary to develop CO_2 capture technologies with as little energy penalty as possible. Typically, a flue gas contains N_2 (75–76%), CO_2 (15–16%), H_2O (5–7%), O_2 (3–4%), CO (20 ppm), SO_x (<800 ppm), and NO_x (<500 ppm) with the emission temperatures of 50–75 °C at 1 bar but its exact composition highly depends on the design of the power plant and the source of natural gas or coal.[4] To capture CO_2 at such concentration requires separating CO_2 in the presence of N_2 and H_2O in post-combustion systems. Known CO_2 separations in a post-combustion process are amine scrubbing (amine washing) and chilled ammonia technologies[5] in which the Lewis acid CO_2 interacts with Lewis basic solution resulting in carbamate formation. Drawbacks include regeneration, fouling of the equipment and solvent boil-off. Alternative methods, *e.g.*, chemisorption on solid oxide surfaces or physical adsorption on porous solids, are attracting increasing attention.

Solid adsorbents are zeolites,[6] metal–organic frameworks (MOFs),[4] silica,[7] activated carbons[8] and porous organic polymers (POPs).[9] MOFs and POPs have gained attention due to their high surface area, ability to be functionalized and selectivity for CO_2 over other gases. Classes of POPs are often differentiated according to their building units such as benzimidazole-linked polymers (BILPs),[10] hyper-crosslinked polymers (HCPs),[11] polymers of intrinsic microporosities (PIMs),[12] porous aromatic frameworks (PAFs),[13] conjugated microporous polymers (CMPs),[14] covalent organic frameworks (COFs),[15] Schiff base networks (SNWs),[16] covalent imine polymers (CIP),[17] porous polymer frames/networks (PPFs/PPNs),[18] element–organic frameworks (EOFs)[19] and nitrogen-doped porous carbon materials (NPCs).[20] POPs often have higher stability towards moisture than MOFs which is crucial for post-combustion CO_2 capture materials.

Covalent triazine-based frameworks (CTFs) are another subclass of POPs that possess high chemical and thermal stability with a high specific surface area.[21] CTFs are interesting because of cheap and readily available starting materials, nitrogen content, facile synthesis and certain hydrophilicity. The following strategies for porous CTF preparation have been reported: (1) ionothermal conditions ($ZnCl_2$),[21] (2) strong Brønsted acid conditions (CF_3SO_3H),[22] and (3) Friedel–Crafts ($AlCl_3$) reaction.[23,24] Kuhn, Antonietti and Thomas *et al.* developed CTFs with permanent porosity.[21] By (1) and (2) these materials are made by the trimerization reaction of carbonitriles to form triazine rings. From their elemental composition, we view CTFs from ionothermal reaction with $ZnCl_2$ as in-between well-defined COFs and porous carbon materials. CTFs with surface areas of up to 1152 $m^2\ g^{-1}$ were synthesized by using strong Brønsted acid conditions (CF_3SO_3H) under room temperature and microwave conditions.[22] Brønsted acid conditions usually provide lower surface areas but they avoid decomposition and condensation reactions such as C–H bond cleavage and carbonization and, hence, result in less structural defects. Recently, anhydrous aluminum chloride catalyzed Friedel–Crafts reactions have been used to prepare rather well-

[a]Institut für Anorganische Chemie und Strukturchemie, Heinrich-Heine-Universität Düsseldorf, 40204 Düsseldorf, Germany. E-mail: janiak@uni-duesseldorf.de

[b]Department of Organic Chemistry, Nanochemistry and Fine Chemistry Research Institute (IUIQFN), Faculty of Sciences, University of Córdoba, Campus de Rabanales, Marie Curie Building, Ctra. Nnal. IV, 14071 Córdoba, Spain

† Electronic supplementary information (ESI) available: Synthesis, NMR, powder XRD, elemental analysis, IR, TGA, gas sorption and selectivity. See DOI: 10.1039/c6ta00638h

defined CTF materials with surface areas up to 1452 $m^2\ g^{-1}$.[23,24] Friedel–Crafts catalysis offers the significant advantages of cheap, easy handling, low reaction temperature, facile synthesis conditions and high yield materials with high surface areas.

Here, the porous frameworks CTF-TPC and CTF-FL were synthesized by Friedel–Crafts reactions between the "linkers" triptycene or fluorene with cyanuric chloride as the "node" in the presence of anhydrous $AlCl_3$ as the catalyst in dichloromethane (Scheme 1, see ESI† for details). After purification, the insoluble materials (Fig. S1 in the ESI†) were reproducibly collected in yields greater 80%. The strong triazine electrophile formed by $AlCl_3$, results in the electrophilic aromatic substitution on triptycene or fluorene to give the triazine frameworks. Network formation was supported by FT-IR (Fig. 1) and ^{13}C MAS or ^{13}C cross-polarization with magnetic angle spinning (CP-MAS) NMR spectroscopy (Fig. S2 and S3, ESI†). The absence of a C–Cl stretching band at 849 cm^{-1} suggested that there was no cyanuric chloride left in the materials.[24] The absorption band of the triazine ring is shifted from 1352 cm^{-1} in cyanuric chloride to 1384 cm^{-1} in CTF-TPC and 1346 cm^{-1} in CTF-FL (see Section 6 in the ESI† for comparative literature data).[25]

The signals in the solid-state ^{13}C CP/MAS NMR spectra are in the expected range (Fig. S2 and S3, ESI†),[26–28] which suggests the formation of triazine-based frameworks. CTF-TPC shows a chemical shift at 51 ppm, corresponding to the bridgehead carbons of the triptycene unit. The signals of the phenyl ring of triptycene are in the range of 120–150 ppm, the triazine ring carbons appear at 164 ppm. CTF-FL shows a peak at 37 ppm,

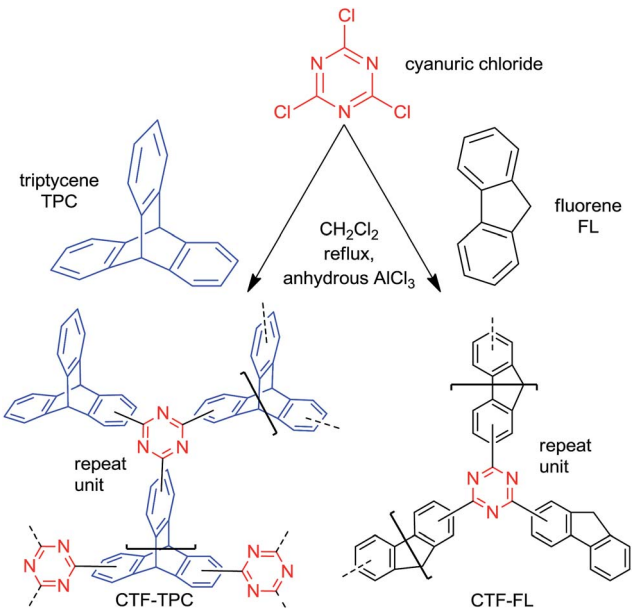

Scheme 1 Synthesis route and model structures for CTF-TPC and CTF-FL (based on elemental analysis, see Section 5 in the ESI†). Both models have a terminal and two bridging ligands for each triazine C_3N_3 ring. For CTF-TPC we do not assume the formation of a symmetric network because of the different possible positions for acylation on the TPC aryl rings. For CTF-FL we assume the formation of a polymer chain which can be crosslinked if the terminal FL occasionally also becomes bridged.

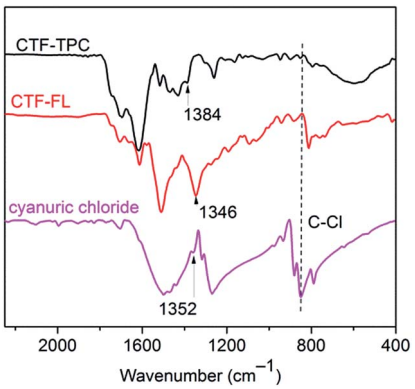

Fig. 1 FT-IR spectra of CTF-TPC and CTF-FL in comparison to that of cyanuric chloride, with proposed triazine bands labelled.

which can be assigned to the methylene bridge carbon in the fluorene unit. The other major peaks from 115 ppm to 150 ppm correspond to the aromatic carbons in the fluorene unit; a peak for the triazine ring carbons is detected at 172 ppm.

The amorphous nature of the products was assessed by PXRD (Fig. S4, ESI†). The diffractograms show only three broad bands around 17, 30 and 40° 2theta. From TGA, it can be observed that CTF-TPC and CTF-FL start to decompose under an O_2 atmosphere at 380 and 360 °C, respectively (Fig. S5, ESI†). Scanning electron microscopy (SEM) reveals aggregation of spherical particles (Fig. 2).

The porosities of the activated CTFs (degassing at 200 °C for 24 h) were characterized by N_2 sorption measurements at 77 K. The N_2 adsorption isotherm of CTF-TPC exhibits a steep increase in N_2 uptake at low p/p_0 values, and continues to increase at high pressure values. Therefore, the curve could be classified as a combination of types I and IV. The H_4 type hysteresis is often associated with narrow slit-like pores but the type I character indicates microporosity.[29] On the other hand, the isotherm of CTF-FL is only of type I with H_4 type hysteresis. The Brunauer–Emmett–Teller (BET) surface areas (pressure range of $p/p_0 = 0.01$–0.05) of CTF-TPC and CTF-FL are 1668 and 773 $m^2\ g^{-1}$, respectively. BET measurements of three other batches each confirmed the reproducibility of the results

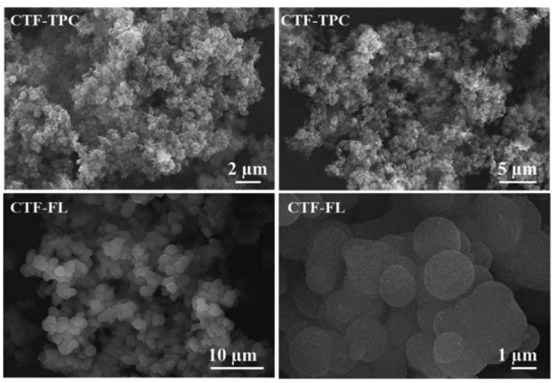

Fig. 2 Scanning electron micrographs (SEM) of CTF-TPC and CTF-FL.

Table 1 Porosity data for CTF-TPC and CTF-FL

Compound	S_{BET}[a] ($m^2\ g^{-1}$)	S_{Lang}[b] ($m^2\ g^{-1}$)	$V_{0.1}$[c] ($cm^3\ g^{-1}$)	V_{tot}[d] ($cm^3\ g^{-1}$)	$V_{0.1}/V_{tot}$	$V_{micro}(CO_2)$[e] ($cm^3\ g^{-1}$)
CTF-TPC	1668	2041	0.65	0.93	0.70	0.11
CTF-FL	773	936	0.31	0.39	0.79	0.11

[a] Calculated BET surface area over the pressure range of 0.01–0.05p/p_0 values for batches from repeated syntheses are given in Table S4 in the ESI. [b] Langmuir surface area over the pressure range of 0–110 torr. [c] Micropore volume calculated from the N_2 adsorption isotherm at $p/p_0 = 0.1$ for pores ≤2 nm (20 Å). [d] Total pore volume at $p/p_0 = 0.95$ for pores ≤20 nm. [e] Total pore volume for pores with diameters smaller than 1 nm (10 Å, *cf.* Fig. S7, ESI) from the CO_2 NL-DFT model at 273 K.

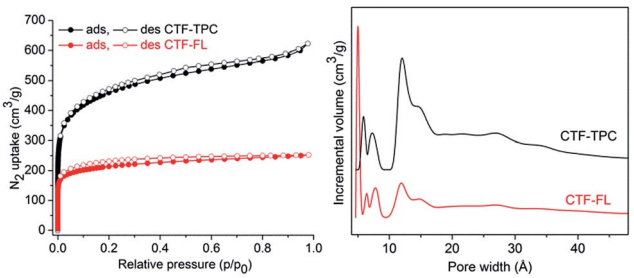

Fig. 3 Nitrogen adsorption–desorption isotherms at 77 K (left) of CTF-TPC and CTF-FL and NLDFT pore size distribution (PSD) curve (right) of CTF-TPC and CTF-FL.

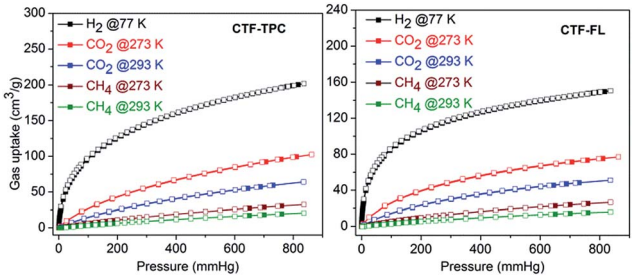

Fig. 4 Gas sorption isotherms of CTF-TPC (left) and CTF-FL (right) (filled symbols for adsorption, empty symbols for desorption).

(Table S4, ESI†). The surface areas are comparable with those of other CTFs (Table S8, ESI†). To the best of our knowledge, the surface area of CTF-TPC, synthesized by $AlCl_3$, exceeds all reported values for similar networks. The surface area of CTF-FL is lower than that of the previously reported fluorene-based CTFs synthesized by $ZnCl_2$.[27] In agreement with the type I isotherms the ratio of micropore volume to total pore volume ($V_{0.1}/V_{tot}$) is in the range of 70–79% (Table 1). Pore size distributions by non-local density functional theory (NLDFT) using the model of "N_2 on carbon, slit-pores method" gave a narrow distribution of micropores centered at 5.9, 7.3, 11.8 and 14.8 Å for CTF-TPC, and 5, 6.4, 8 and 11.8 Å for CTF-FL (Fig. 3). However, a low proportion of mesopores was observed around ~27 Å for both CTFs in agreement with the H_4 hysteresis of the N_2 isotherms.

The H_2 sorption of CTF-TPC and CTF-FL (Table 2 and Fig. 4) is comparable to that of many reported CTF materials.[21a,27,30,31] The CO_2 adsorption of 95.2 $cm^3\ g^{-1}$ (4.24 mmol g^{-1}) for CTF-TPC and of 73.2 $cm^3\ g^{-1}$ (3.26 mmol g^{-1}) for CTF-FL (Tables 2 and S5, ESI†) agrees with the published data for other CTFs such as FL-CTF (1.27–4.28 mmol g^{-1}),[26a] FCTF-1 (4.67–5.53 mmol g^{-1}),[32] CTF-0 (4.22 mmol g^{-1}),[33] CTF-1 (2.47–3.82 mmol g^{-1}),[32] CTF-Pl–P6 (1.88–3.39 mmol g^{-1}),[22] CTF-P1M–P6M (0.94–4.42 mmol g^{-1}),[22] MCTF-300–500 (2.25–3.16 mmol g^{-1}),[34] PCTF-1–7 (1.85–3.26 mmol g^{-1})[31] and NOP-1–6 (1.31–2.51 mmol g^{-1})[30] (see Table S8 in the ESI† for details). The isosteric heats of adsorption (Q_{st}) from the CO_2 adsorption isotherms at 273 and 298 K near zero loading are 32 and 35 kJ mol^{-1} for CTF-TPC and -FL, respectively (Fig. S6, ESI†), and are again comparable to those of other CTFs (see Section 11 in the ESI†). Upon increasing the loading the Q_{st} values decrease to 26 and 28 kJ mol^{-1} for CTF-TPC and CTF-FL, respectively, which are, however, still well above the heat of liquefaction of bulk CO_2 with 17 kJ mol^{-1}. The high Q_{st} value can be attributed to the high polar framework and the pore size effect. The high adsorption enthalpy at zero coverage is explained by the initial filling of the small ultramicropores with 4 Å diameter (Fig. S7†) with adsorbate–surface interactions to both sides or ends of the CO_2 molecules.

The CH_4 uptake capacities of CTF-TPC and CTF-FL (Fig. 4, Tables 2 and S5 in the ESI†) are comparable with the values for PCTF-1 to -7 from our previous work as well as other CTFs.[24,31] The gas sorption capacity for CH_4 of CTFs follows the increase in surface area and pore volume (Table 1).

Table 2 Gas uptake at 1 bar and selectivity data for CTF-TPC and CTF-FL

Compound	H_2[a] ($cm^3\ g^{-1}$)	CO_2[b] ($cm^3\ g^{-1}$)	$Q^0_{ads}(CO_2)$[c] (kJ mol^{-1})	CH_4[b] ($cm^3\ g^{-1}$)	N_2[b] ($cm^3\ g^{-1}$)	$CO_2 : N_2$[d] Henry	$CO_2 : N_2$[d] IAST
CTF-TPC	195.8	95.2	32	30	9.2	20	30
CTF-FL	146.6	73.2	35	24.9	7.1	25	48

[a] Gas uptake at 77 K. [b] At 273 K. [c] Heat of adsorption for CO_2 at zero loading from adsorption isotherms acquired at 273 and 293 K. [d] Gas selectivity calculated at 273 K.

From the available single-gas adsorption isotherms, the CO_2 selectivities over N_2 or CH_4 for CTF-TPC and CTF-FL were calculated at 273 and 293 by using the Henry equation and the ideal adsorbed solution theory (IAST). From the Henry equation, the adsorption selectivity for CO_2 over N_2 is 20 and 25 at 273 K (16 and 21 at 293 K) for CTF-TPC and CTF-FL, respectively, whereas the corresponding CO_2/CH_4 selectivities were in the range of 4–5 at 273 K and 293 K (Fig. S8 and S9 in the ESI; Tables 2 and S5 in the ESI†). From IAST (Fig. S10, S11 and Tables S6, S7 in the ESI†), the CO_2/N_2 selectivities of CTF-TPC and CTF-FL are 30 and 48 at 273 K (Table 2), which are higher than from the Henry calculation. The selectivity of CTF-FL is high compared with recent work by others.[27] A trade-off relation is observed for the CO_2/N_2 selectivity *versus* porosity: a higher surface area of CTF-TPC (compared to CTF-FL) exhibits lower selectivity, as can be generalized for other CTF-based polymers (see Table S8 in the ESI†).

In summary, the $AlCl_3$ catalyzed Friedel–Crafts reaction can be used for the aromatic linkers triptycene and fluorene to construct triazine-based frameworks. By using this approach, the compound CTF-TPC with 1668 $m^2 g^{-1}$ gave the highest BET surface area found for such $AlCl_3$-catalyzed cyanuric-chloride based CTFs, so far. It is suggested that the triptycene unit is especially amenable to construct high surface-area porous materials.[35] CTF-TPC and CTF-FL adsorbed 4.24 mmol g^{-1} and 3.26 mmol g^{-1} (273 K/1 bar) of CO_2, respectively. Such high CO_2 uptake together with cost-effective synthesis make CTFs a promising candidate for porous adsorbents. Porosity and gas adsorption behavior can be tuned by changing the linker in this cyanuric-acid/$AlCl_3$-catalysis approach.

Acknowledgements

Support of the work by BMBF project OptiMat 03SF0492C and by the University of Düsseldorf through its strategic research fund (SFF) is gratefully acknowledged. We thank Mrs J. Dechnik, Mrs L. Schmolke, Mr D. Dietrich, Mr S. Glomb, Mr Hastürk and Mr P. Roloff for their help in analytical measurements.

Notes and references

1 R. S. Haszeldine, *Science*, 2009, **325**, 1647.
2 K. Sumida, D. L. Rogow, J. A. Mason, T. M. McDonald, E. D. Bloch, Z. R. Herm, T.-H. Bae and J. R. Long, *Chem. Rev.*, 2012, **112**, 724–781; H. He, W. Li, M. Zhong, D. Konkolewicz, D. Wu, K. Yaccato, T. Rappold, G. Sugar, N. E. David and K. Matyjaszewski, *Energy Environ. Sci.*, 2013, **6**, 488–493.
3 D. M. D'Alessandro, B. Smit and J. R. Long, *Angew. Chem., Int. Ed.*, 2010, **49**, 6058–6082.
4 J. A. Mason, T. M. McDonald, T.-H. Bae, J. E. Bachman, K. Sumida, J. J. Dutton, S. S. Kaye and J. R. Long, *J. Am. Chem. Soc.*, 2015, **137**, 4787–4803.
5 G. T. Rochelle, *Science*, 2009, **325**, 1652–1654; U. Desideri and A. Paolucci, *Energy Convers. Manage.*, 1999, **40**, 1899–1915.
6 J. Zhang, P. A. Webley and P. Xiao, *Energy Convers. Manage.*, 2008, **49**, 346–356.
7 (*a*) G. Qi, Y. Wang, L. Estevez, X. Duan, N. Anako, A.-H. A. Park, W. Li, C. W. Jones and E. P. Giannelis, *Energy Environ. Sci.*, 2011, **4**, 444–452; (*b*) J. C. Hicks, J. H. Drese, D. J. Fauth, M. L. Gray, G. Qi and C. W. Jones, *J. Am. Chem. Soc.*, 2008, **130**, 2902–2903.
8 L. Wang and R. T. Yang, *J. Phys. Chem. C*, 2012, **116**, 1099–1106.
9 V. Guillerm, L. J. Weselinski, M. Alkordi, M. I. H. Mohideen, Y. Belmabkhout, A. J. Cairns and M. Eddaoudi, *Chem. Commun.*, 2014, **50**, 1937–1940; S. Mondal and N. Das, *J. Mater. Chem. A*, 2015, **3**, 23577–23586; G. Liu, Y. Wang, C. Shen, Z. Ju and D. Yuan, *J. Mater. Chem. A*, 2015, **3**, 3051–3058.
10 M. G. Rabbani and H. M. El-Kaderi, *Chem. Mater.*, 2012, **24**, 1511–1517.
11 J. Germain, J. Hradil, J. M. J. Fréchet and F. Svec, *Chem. Mater.*, 2006, **18**, 4430–4435.
12 B. S. Ghanem, K. J. Msayib, N. B. McKeown, K. D. M. Harris, Z. Pan, P. M. Budd, A. Butler, J. Selbie, D. Book and A. Walton, *Chem. Commun.*, 2007, 67–69.
13 H. Zhao, Z. Jin, H. Su, J. Zhang, X. Yao, H. Zhao and G. Zhu, *Chem. Commun.*, 2013, **49**, 2780–2782.
14 J.-X. Jiang, F. Su, A. Trewin, C. D. Wood, N. L. Campbell, H. Niu, C. Dickinson, A. Y. Ganin, M. J. Rosseinsky, Y. Z. Khimyak and A. I. Cooper, *Angew. Chem., Int. Ed.*, 2007, **46**, 8574–8578.
15 (*a*) S.-Y. Ding and W. Wang, *Chem. Soc. Rev.*, 2013, **42**, 548–568; (*b*) Introduction to themed issue on COFs: A. I. Cooper, *CrystEngComm*, 2013, **15**, 1483; (*c*) S. Kandambeth, A. Mallick, B. Lukose, M. V. Mane, T. Heine and R. Banerjee, *J. Am. Chem. Soc.*, 2012, **134**, 19524–19527; (*d*) T. Ben, H. Ren, S. Ma, D. Cao, J. Lan, X. Jing, W. Wang, J. Xu, F. Deng, J. M. Simmons, S. Qiu and G. Zhu, *Angew. Chem., Int. Ed.*, 2009, **48**, 9457–9460; (*e*) S. Dalapati, S. Jin, J. Gao, Y. Xu, A. Nagai and D. Jiang, *J. Am. Chem. Soc.*, 2013, **135**, 17310–17313; (*f*) S. Nandi, U. Werner-Zwanziger and R. Vaidhyanathan, *J. Mater. Chem. A*, 2015, **3**, 21116–21122.
16 M. Shunmughanathan, P. Puthiaraj and K. Pitchumani, *ChemCatChem*, 2015, **7**, 666–673.
17 R. Gomes, P. Bhanja and A. Bhaumik, *Chem. Commun.*, 2015, **51**, 10050–10053.
18 L.-B. Sun, A.-G. Li, X.-D. Liu, X.-Q. Liu, D. Feng, W. Lu, D. Yuan and H.-C. Zhou, *J. Mater. Chem. A*, 2015, **3**, 3252–3256.
19 M. Rose, W. Bohlmann, M. Sabo and S. Kaskel, *Chem. Commun.*, 2008, 2462–2464.
20 M. Nandi, K. Okada, A. Dutta, A. Bhaumik, J. Maruyama, D. Derks and H. Uyama, *Chem. Commun.*, 2012, **48**, 10283–10285.
21 (*a*) P. Kuhn, M. Antonietti and A. Thomas, *Angew. Chem., Int. Ed.*, 2008, **47**, 3450–3453; (*b*) P. Kuhn, A. l. Forget, D. Su, A. Thomas and M. Antonietti, *J. Am. Chem. Soc.*, 2008, **130**, 13333–13337.
22 S. Ren, M. J. Bojdys, R. Dawson, A. Laybourn, Y. Z. Khimyak, D. J. Adams and A. I. Cooper, *Adv. Mater.*, 2012, **24**, 2357–2361.

23 H. Lim, M. C. Cha and J. Y. Chang, *Macromol. Chem. Phys.*, 2012, **213**, 1385–1390.
24 P. Puthiaraj, S.-M. Cho, Y.-R. Lee and W.-S. Ahn, *J. Mater. Chem. A*, 2015, **3**, 6792–6797.
25 (*a*) S. K. Kundu and A. Bhaumik, *RSC Adv.*, 2015, **5**, 32730–32739; (*b*) C. Bai, M. Zhang, B. Li, Y. Tian, S. Zhang, X. Zhao, Y. Li, L. Wang, L. Ma and S. Li, *J. Hazard. Mater.*, 2015, **300**, 368–377; (*c*) P. Puthiaraj, S.-S. Kim and W.-S. Ahn, *Chem. Eng. J.*, 2016, **283**, 184–192.
26 (*a*) C. Zhang, Y. Liu, B. Li, B. Tan, C.-F. Chen, H.-B. Xu and X.-L. Yang, *ACS Macro Lett.*, 2012, **1**, 190–193; (*b*) C. Zhang, T.-L. Zhai, J.-J. Wang, Z. Wang, J.-M. Liu, B. Tan, X.-L. Yang and H.-B. Xu, *Polymer*, 2014, **55**, 3642–3647.
27 S. Hug, M. B. Mesch, H. Oh, N. Popp, M. Hirscher, J. Senker and B. V. Lotsch, *J. Mater. Chem. A*, 2014, **2**, 5928–5936.
28 S. Kuecken, J. Schmidt, L. Zhi and A. Thomas, *J. Mater. Chem. A*, 2015, **3**, 24422–24427.
29 M. Thommes, K. Kaneko, A. V. Neimark, J. P. Olivier, F. Rodriguez-Reinoso, J. Rouquerol and K. S. W. Sing, *Pure Appl. Chem.*, 2015, **87**, 1051–1069.
30 S. Xiong, X. Fu, L. Xiang, G. Yu, J. Guan, Z. Wang, Y. Du, X. Xiong and C. Pan, *Polym. Chem.*, 2014, **5**, 3424–3431.
31 (*a*) A. Bhunia, V. Vasylyeva and C. Janiak, *Chem. Commun.*, 2013, **49**, 3961–3963; (*b*) A. Bhunia, I. Boldog, A. Möller and C. Janiak, *J. Mater. Chem. A*, 2013, **1**, 14990–14999.
32 Y. Zhao, K. X. Yao, B. Teng, T. Zhang and Y. Han, *Energy Environ. Sci.*, 2013, **6**, 3684–3692.
33 P. Katekomol, J. Roeser, M. Bojdys, J. Weber and A. Thomas, *Chem. Mater.*, 2013, **25**, 1542–1548.
34 X. Liu, H. Li, Y. Zhang, B. Xu, S. A, H. Xia and Y. Mu, *Polym. Chem.*, 2013, **4**, 2445–2448.
35 (*a*) G. Zhang, O. Presly, F. White, I. M. Oppel and M. Mastalerz, *Angew. Chem., Int. Ed.*, 2014, **53**, 1516–1520; (*b*) G. Zhang, O. Presly, F. White, I. M. Oppel and M. Mastalerz, *Angew. Chem., Int. Ed.*, 2014, **53**, 5126–5130; (*c*) S. M. Elbert, F. Rominger and M. Mastalerz, *Chem.–Eur. J.*, 2014, **20**, 16707–16720.